Automated Framework for the Optimisation of Spatial Layouts for Concrete Structures Reinforced with Robotic Filament Winding

R. Oval[a], E. Costa[b], D. Thomas-McEwen[a], S. Spadea[c], J. Orr[a], P. Shepherd[b]

[a]Department of Engineering, University of Cambridge, United Kingdom
[b]Department of Architecture and Civil Engineering, University of Bath, United Kingdom
[c]School of Science and Engineering, University of Dundee, United Kingdom

rpho2@cam.ac.uk

Abstract -

Concrete is a major contributor to the environmental impact of the construction industry, due to its cement content but also its reinforcement. Reinforcement has a significant contribution because of construction rationalisation, resorting to regular mats or cages of steel bars, despite layout-optimisation algorithms and additive-manufacturing technologies. This paper presents an automated framework, connecting design and fabrication requirements for the optimisation of spatial layouts as of reinforcement of concrete structures, by the means of robotic filament winding.

Keywords -

Automated construction; Concrete structures; Reinforced concrete; Strut-and-tie models; Layout optimisation; Wound reinforcement; Digital fabrication; Additive manufacturing; Robotics; Robotic filament winding; 3D winding; Coreless winding; Trajectory planning

1 Introduction

This paper presents research on the automated reinforcement of concrete structures, investigated in the framework of the research project *Automating Concrete Construction* (ACORN) [1, 2].

1.1 Context

The construction industry is responsible for nearly 50% of the UK's carbon emissions [3]. More specifically, concrete construction is the main culprit, with more than 5% of the carbon emissions worldwide. The environmental impact of reinforced concrete stems from the amount of cement as well as the amount of reinforcement [4]. Layout optimisation applied to strut-and-tie models can find optimised tensile reinforcement for various concrete elements [5, 6]. However, these optimised layouts are not affordable, or even feasible, without significant post-rationalisation to build such reinforcement from stiff bar elements. Extreme rationalisation resorts to the use of standardised reinforcement bars, mats and cages, which require a higher amount of material and energy to produce. However, the use of advanced fabrication strategies and additive manufacturing, combined with robotics, provides an opportunity to automate the fabrication of complex optimised layouts of reinforced concrete structures using flexible filament materials.

1.2 Literature review

Short fibres can improve durability, provide a minimum tensile reinforcement against cracking and isotropic strengthening [7]. However, short fibres do not reinforce specific directions to carry high local tensile stresses based on an optimised layout. Reinforcement mats can carry higher tensile stresses, but the use of non-optimal, homogeneous and orthogonal meshes demands more material, and their placement is hard to automate, requiring patching and overlapping to map large-span plates or shells with double curvature [8, 9]. High, local, oriented tensile capacity can be provided by long fibres, or filaments [10]. Moreover, filaments are suitable for automated additive manufacturing [11], as commonly proven in the automotive industry to produce composite parts thanks to robotic filament winding [12]. For instance, the technology FibreTEC3D [13, 14], developed by Daimler and CIKONI, winds spatial layouts to produce mechanically-optimised components. In the construction industry, Spadea *et al.* [10] wound shear reinforcement for concrete beams using a rotating mandrel as core and Prado *et al.* [15] wound filaments to form composite shells using robotic arms holding boundary frames, instead of using a core. Filament winding of tensile reinforcement offers the flexibility to produce complex but optimised shapes and is suitable for automation using robotic arms. Moreover, achieving coreless winding removes the constraint of laying the filament on the surface of a core object, whose fabrication can be saved.

1.3 Outline

This paper presents an automated framework for the optimisation of tensile reinforcement for concrete structures that are suitable for robotic filament winding. Section
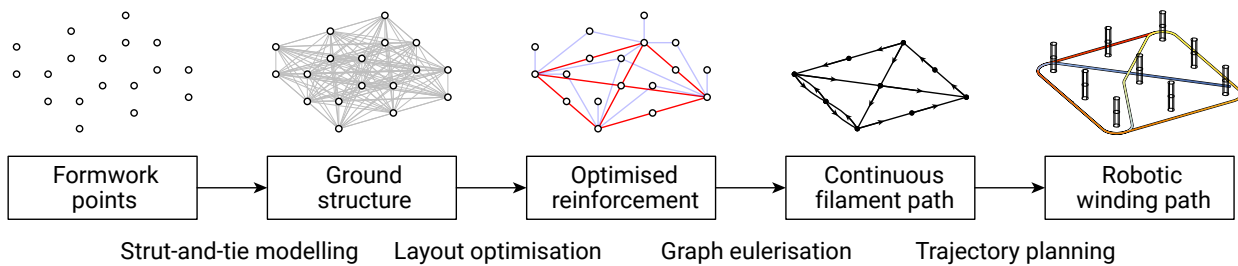
Figure 1. Workflow for the robotic filament winding of tensile reinforcement for concrete structures, including fabrication-informed generation, optimisation and rationalisation.

2 presents the automated framework, taking into account the constraints of the formwork system during the process of structural optimisation and the additive-manufacturing strategy for fabrication rationalisation. Section 3 applies this framework to a standard, benchmark plate with numerical results comparing the material quantities before and after rationalisation.

2 Automated framework

The workflow, illustrated in Figure 1 and detailed in this section, includes structural optimisation and rationalisation informed by fabrication requirements according to the following steps:

1. Define the winding points in the formwork system;

2. Generate a ground structure based on these points, which includes all the admissible winding passes;

3. Optimise the layout of this ground structure to obtain a strut-and-tie model with a minimal amount of tensile reinforcement;

4. Rationalise the tensile layout for robotic filament winding by creating a continuous path using graph Eulerisation;

5. Generate the trajectory for robotic winding around the formwork elements.

2.1 Formwork system

For coreless winding of a spatial layout made of a flexible filament, winding points are necessary for anchoring and deviating the filament and for tensioning it before concreting.

Such winding points can be included in the formwork of any structural system, such as beams, plates or shells, as illustrated in red in Figure 2. These elements must be designed according to the formwork strategy, be it rigid timber frame or flexible membrane, for instance. Stiff pins that can transmit the shear forces of the tensioned filament

to the formwork can be reused, by covering them with a sliding lost cap and by removing them before demoulding, and the resulting void subsequently grouted.

The higher the density of these elements, the more diverse the range of potential reinforcement layouts, although these elements have a cost in terms of production time and material consumption. The position of these winding points serve as input for structural optimisation, informed by the available design space.

2.2 Structural optimisation

The structural design of the reinforcement for concrete structures is based on layout optimisation using a strut-and-tie model.

Strut-and-tie models are discrete stress fields use to design concrete structures as a set of compressive struts and tensile ties for the given support and load conditions. Their justification is based on the lower-bound theorem of plasticity. While concrete plays the role of the compressive struts, the reinforcements act as tensile ties. Structural analysis of the strut-and-tie model provides the stresses and the necessary cross-sections of tensile reinforcement. This model can include any combination of lines connecting the winding points in the formwork system, which can all be built using filament winding.

In this combinatorial design space of tensile ties, some layouts are more efficient and therefore require less reinforcement. The search through this space of feasible layouts is performed using layout optimisation [16, 17]. Such methods minimise the amount of material, which is equivalent to the total load path LP, which is the sum of the force F_i times the length L_i in each edge i over the entire set of edges E:

$$LP = \sum_{i \in E} |F_i| L_i$$

.

Minimising the amount of tensile reinforcement is equivalent to minimising this load path, when the location, magnitude and direction of the external forces is the
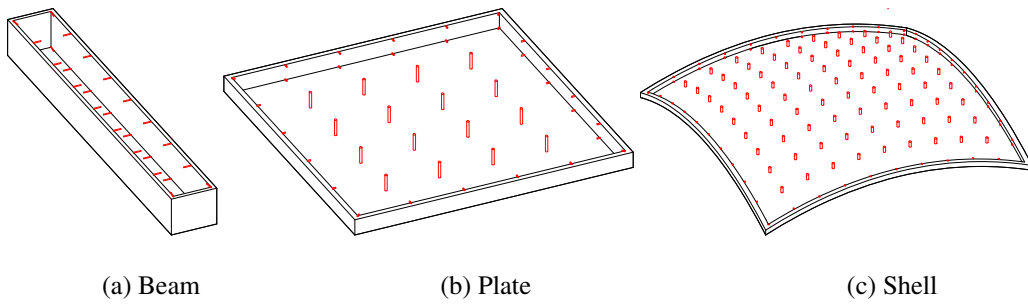
(a) Beam   (b) Plate   (c) Shell

Figure 2. Formwork system with winding points, using elements in red to anchor and deviate the flexible filament.

same. Indeed, according to Maxwell's theorem [18], the algebraic load path, which comprises the tensile part T and the compressive part C, only depends on the applied loads:

$$\sum |F_T| L_T - \sum |F_C| L_C = \sum \underline{\mathbf{P}} \cdot \underline{\mathbf{r}},$$

with $\underline{\mathbf{P}}$ the external loads and $\underline{\mathbf{r}}$ their position vectors from any arbitrary reference point. Since the algebraic load path is constant for a given set of loads, decreasing the total volume of material decreases in equal volume the compression material and the tension material.

Therefore, global layout optimisation provides the minimum reinforcement.

After optimisation, the discrete cross-section A_f of the filament must be included. For each tensile element, the force F_T is retrieved to find the necessary number n of filament passes that must constitute this element to take this force, based on the filament tensile strength f_f:

$$n = \left\lceil \frac{F}{A_f \cdot f_f} \right\rceil.$$

The lower the filament cross-section, the lower the loss of material due to the rounding up and oversizing, but the higher the number of passes and the production time.

As the initial ground structure was informed by the location of the winding points in the formwork, the resulting structurally-optimised layouts include only passes that can be realised by the filament. Even though significant post-processing is not necessary, a rationalisation step is required to obtain a continuous path through the tensile reinforcement layout. This specific continuity requirement prevents from multiple interruptions of the filament-based fabrication process, whether manually or robotically wound.

2.3 Fabrication rationalisation

From the optimised layout, a continuous path for filament winding must be computed that respects the required number of passes per tensile element. From this continuous path, a robotic trajectory is generated that winds the reinforcement around the winding points of the formwork.

However, the existence of such a continuous path is not guaranteed for any graph of nodes and edges. Here, the graph consists of the winding points as nodes and the tensile elements as edges. Since some edges require multiple passes to achieve the necessary filament cross-section, the algorithm is applied to a multi-graph, where multiple edges can connect the same pair of nodes. For each pair of nodes requiring n passes, n edges connect the pair of nodes in the graph.

Figure 3a shows an Eulerian graph with a closed circuit, marked with arrows, that visits each edge of the graph exactly once. This strong constraint of a circuit can be relaxed to an open path, as the wound filament does not need to close. Such a graph is called a semi-Eulerian graph, as in Figure 3b with path extremities marked with white nodes. However, some graphs do not have such paths nor circuits, such as the one in Figure 3c.
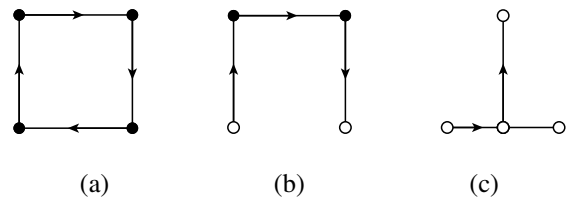

(a)   (b)   (c)

Figure 3. Eulerian properties of graphs: (a) an Eulerian graph with a cycle, (b) a semi-Eulerian graph with a path and (c) a graph without path visiting each edge exactly once.

The problem of finding a path can be solved with Eulerisation algorithms, which convert graphs into Eulerian graphs, which have the property of containing a circuit, or closed path, that visits each edge of the graph exactly once. The Eulerisation problem is also called the Chinese Postman Problem (CPP) [19]. The CPP searches for edges to add to obtain a circuit. In Figure 4, Eulerisation of the graph yields two Eulerian graphs. To minimise the amount

of material for needed reinforcement, the one that corresponds to a minimal length of added edges is retained. This algorithm is adapted to perform semi-Eulerisation to find a continuous path by considering different path extremities, highlighted in white in Figure 5, resulting in more semi-Eulerian graphs, with fewer edges added due to rationalisation.
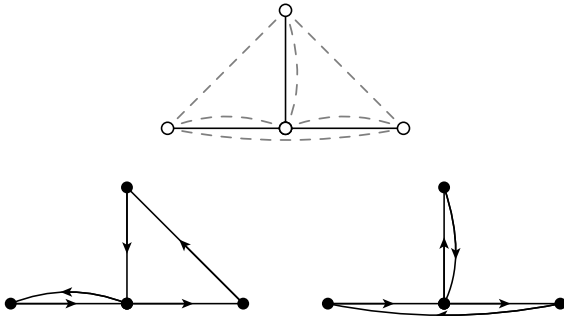

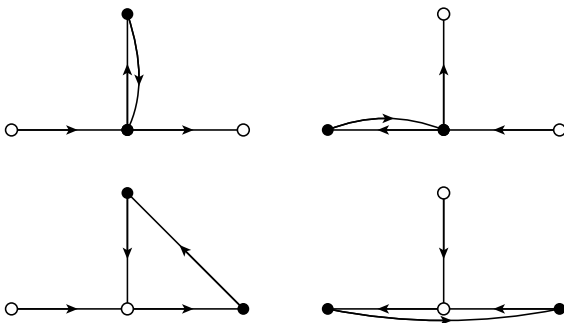Figure 4. Eulerisation of a graph by adding edges to find a closed circuit.

Figure 5. Semi-Eulerisation of a graph by adding edges to find an open path.

However, because the tensile parts can form disconnected graphs, and because other edges in the ground structure represent other potential winding passes, the Rural Postman Problem (RPP) [20] is used, which is a generalisation of the CPP. The RPP, also called priority-constrained CPP, finds a circuit that visits each required edge exactly once and potentially visits optional edges of the graph to form a circuit or path. Here, the required edges are the tensile edges and the optional edges are all the edges of the ground structure.

While the CPP is NP-complete, the RPP is NP-hard. Therefore, multiple algorithms exist to solve this problem based on heuristics. Here, the sub-paths are found for each disconnected component first, using a CPP algorithm. Then, as shown in Figure 6, these sub-paths, simplified as black edges, are iteratively connected in a greedy approach by adding the shortest optional path, highlighted in red,

among all the possible ones, until they form a general path that connects all the sub-paths.

As a result, a continuous path is found through the tensile part of the optimised strut-and-tie model, taking into account the number of passes per edge.

From the continuous path, a trajectory for robotic winding around the formwork points is obtained.

The bulk of the formwork elements informs the offset of the lines connecting the axes of these elements. The orientation of the offset takes into account the relative positions of the elements along the winding path. Figure 7 shows how from a path, in black, connecting winding elements, in white, the trajectory, in red, alternates on the right- and left-hand sides based on the successive path turns. The trajectory passes by the opposite side of the next element: winding from element $i-1$ to i, the filament goes to the right-hand side of the path at the element i if the next element $i+1$ is on the left-hand side, and vice versa.

Vertical sliding along the elements is assumed to be prevented.

The robotic trajectory computation completes this automated workflow to obtain an optimised layout to wind reinforcement in concrete structures around formwork points.

3 Structural application

This automated workflow is applied to a classic plate as a benchmark, though more complex shapes can be considered, as long as winding points are provided during the fabrication process.

3.1 Parameters

The plate is a 5m x 5m square, has a thickness of 20cm, is supported vertically at its bottom four corners and is loaded at the top surface with a uniform downward vertical load of 5 kN/m^2. The concrete is considered to be C30/37 with a compressive strength f_c=30MPa. The filament is considered to be Fibre-Reinforced Polymer with a tensile strength f_f=1500MPa and a cross-section A_f=4.3mm^2 [21]. The winding points in the formwork are organised in a 6 x 6 x 2 array of 72 nodes, corresponding to a spacing of 1m in-plane and 0.2m vertically, as shown in Figure 8 with the results of the automated workflow.

3.2 Results

The ground structure, shown in grey in Figure 8a, connects all the pairs of the 72 winding points, highlighted as white dots, to each other, representing all the $\binom{72}{2}$=2556 edges that can be potential filament paths. Only edges shorter than 3m are shown for clarity.

The optimised strut-and-tie model in Figure 8b shows the support reactions in green, the external loads in orange,
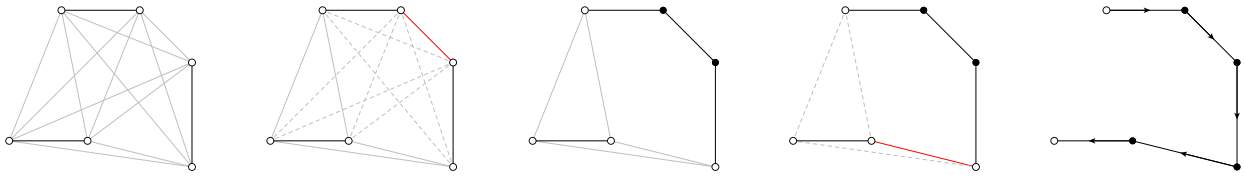
Figure 6. Semi-Eulerisation of a disconnected graph by finding first sub-paths, in black, and then connecting them with the shortest optional paths, in red.
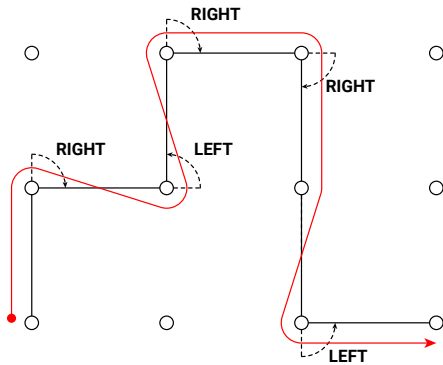

Figure 7. Winding trajectory, in red, from the filament path, in black, alternating between the right- and left-hand sides.

the compressive struts in blue and the tensile ties in red. The cylindrical elements are sized based on the internal forces and corresponding material strengths. The tensile load path amounts to 3266kN.m, or a theoretical material volume of CFRP of 0.00218m^3. A grid of winding points with an XY spacing of 50cm gives 3004kN.m, or 8% less, and an XY spacing of 25cm gives 2870kN.m, or 12% less, but also more than 3 times and 12 times the number of formwork elements, respectively. These results are summarised in Table 1.

Table 1. Tensile load paths for different densities of formwork winding points

winding node spacing [cm]	tensile load path [kN.m]	nb. of winding nodes [-]
100	3266 (100%)	72
50	3004 (92%)	242
25	2870 (88%)	882

Once computed the number of passes per tensile element, the filament volume is 0.00241m^3, an increase of 11%, for a total filament length of 561m. The graph in Figure 8c illustrates the continuous filament path generated after semi-Eulerisation. The colours and thicknesses illustrate the number of passes per edge, ranging from thin green edges with 1 pass to thick red edges with 10 passes.

The filament volume is then 0.00246m^3, an additional increase of 2%, for a total filament length of 572m that can be wound in one go. Eventually, the total increase of material volume from the initial, optimal strut-and-tie model including the winding points to the filament path amounts to 13%. Table 2 summaries the material quantities at the different steps of the optimisation and rationalisation workflow.

The continuous curve in Figure 8d represents the path of the extremity of the robot end-effector winding the filament around the formwork elements. The path time is plotted as a colour gradient from red to blue, from an extremity to the other of the job. The material increase due to the bulkiness of the formwork elements is not taken into account.

Table 2. Reinforcement material quantities after each step of the optimisation and rationalisation workflow

step	volume [m^3]	increase [-]
layout optimisation	0.00218	-
discrete sizing	0.00241	+11%
graph eulerisation	0.00246	+2%
total		+13%

3.3 Discussion

This case study shows the application of a digital framework for the optimisation of structurally-sound and fabrication-informed reinforcement layouts. The numerical results predicting the material quantities highlight the trade-offs between the theoretical optimal design and the feasible sub-optimal design. The waste of material due to winding (2%) is low compared to the waste due to using a limited number of winding points in the formwork (around 10%) and compared to oversizing due to the use of a single cross-section for the filament (11%). These parameters, number of winding points and discrete filament cross-section, also have an impact on the production time, due to assembly/disassembly time of the formwork and winding time of the robot, respectively. A physical prototype of a structural element with a specific formwork system will allow the evaluation of this impact. The specific setup will introduce additional constraints, related to

(a) Ground structure

(b) Strut-and-tie model

SUPPORT REACTIONS
EXTERNAL LOADS
COMPRESSIVE STRUTS
TENSILE TIES

1 PASS ● ● ● **10 PASSES**

(c) Connectivity graph

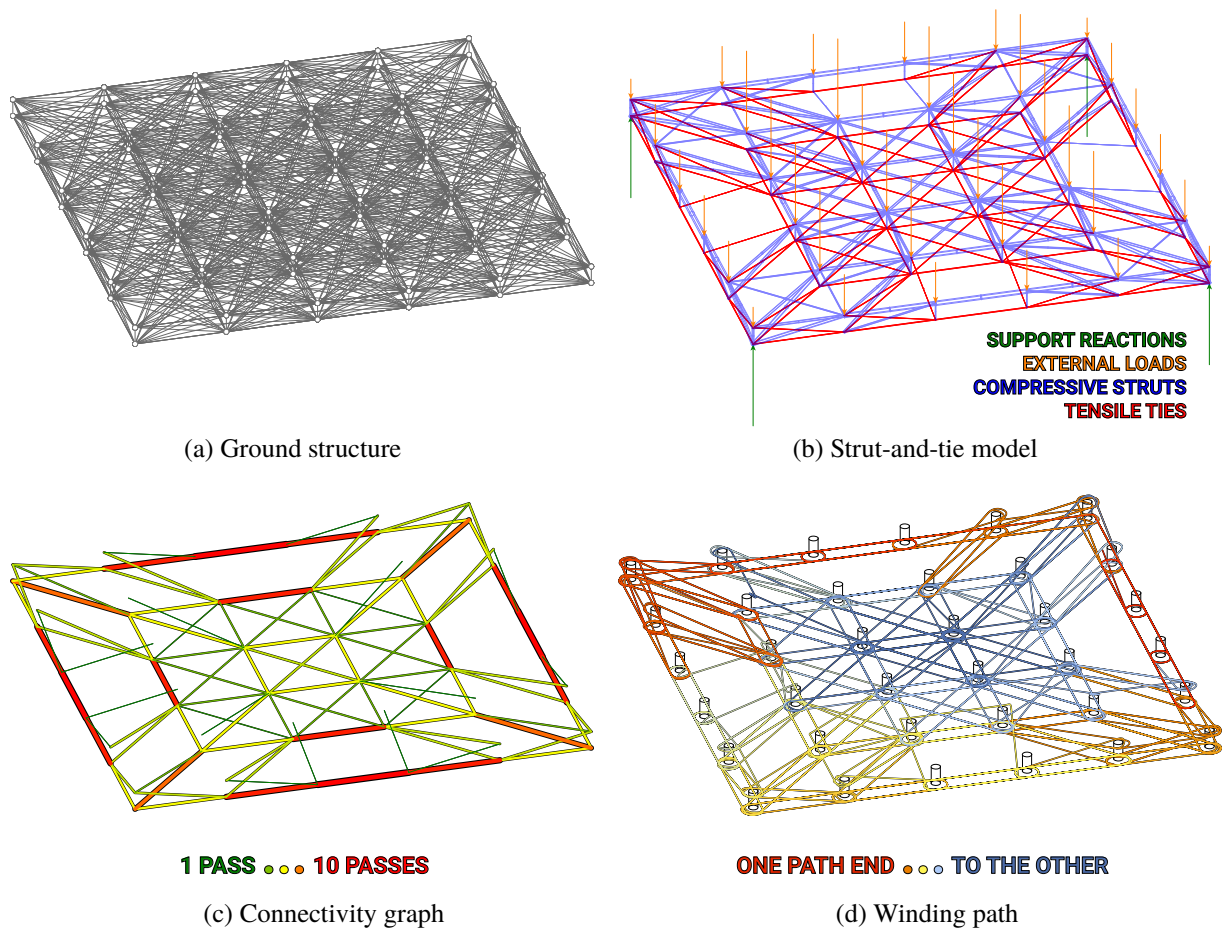**ONE PATH END** ● ● ● **TO THE OTHER**

(d) Winding path

Figure 8. Automated optimisation and rationalisation of a reinforcement layout suitable for robotic filament winding applied to a concrete plate of 5m x 5m x 20cm.

reach possibilities and the collision risks, which will need to be integrated into this automated workflow.

4 Conclusion

Advanced fabrication technology should enable the production of optimised reinforcements, instead of resorting to standardised and inefficient cages or mats, which significantly contribute to the environmental impact of reinforced-concrete structures. This paper presented an automated framework for the design of optimised reinforcement layouts for concrete structures that are suitable for robotic filament winding. Its application to a reinforced-concrete slab highlight the impact of the rationalisation steps and some of their parameters. Further work consists of:

- parametric studies on the spacing of the formwork points for winding, the filament cross-section, as well as layout simplification, to reduce the production time

with controlled deviation from the optimal tensile reinforcement;

- physical prototypes with detailing of the formwork system and its winding points, exact generation of the robotic tool-path and inverse kinematics that prevents clashes, with the sequencing of the winding from the bottom layer to the top layer of the reinforcement layout;

- material and structural testing to understand the behaviour of this system, including the bonding between concrete and reinforcement; and

- life-cycle assessment to compare the whole-life cost of this approach with traditional methods, as comparing only embodied material can be misleading, without taking into account production waste and energy.

Acknowledgements

References

[1] ACORN: Automating Concrete Construction, 2019. URL `http://automated.construction/`. Accessed on 15/06/2020.

[2] Eduardo Costa, Paul Shepherd, John Orr, Tim Ibell, and Robin Oval. Automating Concrete Construction: Digital design of non-prismatic reinforced concrete beams. In *2nd RILEM International Conference on Concrete and Digital Fabrication (DigitalConcrete 2020)*, 2020.

[3] Department for Business Innovation & Skills (BIS). Estimating the amount of CO2 emissions that the construction industry can influence - supporting material for the Low Carbon Construction IGT Report, 2010.

[4] Hashem Alhumayani, Mohamed Gomaa, Veronica Soebarto, and Wassim Jabi. Environmental assessment of large-scale 3D printing in construction: A comparative study between cob and concrete. *Journal of Cleaner Production*, 2020.

[5] Jorg Schlaich, Kurt Schäfer, and Mattias Jennewein. Toward a consistent design of structural concrete. *PCI journal*, 1987.

[6] Jackson L Jewett and Josephine V Carstensen. Experimental investigation of strut-and-tie layouts in deep RC beams designed with hybrid bi-linear topology optimization. *Engineering Structures*, 2019.

[7] ACI Committee: State of the art report on fiber reinforced concrete, ACI 544.1R-82. Technical report, American Concrete Institute, Detroit, 2006.

[8] Tomás Méndez Echenagucia, Dave Pigram, Andrew Liew, Tom Van Mele, and Philippe Block. A cable-net and fabric formwork system for the construction of concrete shells: Design, fabrication and construction of a full scale prototype. *Structures*, 2019.

[9] Will Hawkins, John Orr, Paul Shepherd, and Tim Ibell. Design, construction and testing of a low carbon thin-shell concrete flooring system. *Structures*, 2019.

[10] Saverio Spadea, John Orr, Antonio Nanni, and Yuanzhang Yang. Wound FRP shear reinforcement for concrete structures. *Journal of Composites for Construction*, 2017.

[11] Ma Quanjin, MRM Rejab, MS Idris, Nallapaneni Manoj Kumar, and MNM Merzuki. Robotic filament winding technique (RFWT) in industrial application: A review of state of the art and future perspectives. *International Research Journal of Engineering and Technology*, 2018.

[12] Ginger Gardiner. Filament winding, reinvented, 2018. URL `https://www.compositesworld.com/articles/filament-winding-reinvented`. Accessed on 15/06/2020.

[13] Niklas Minsch, Matthias Müller, Thomas Gereke, Aandreas Nocke, and Chokri Cherif. Novel fully automated 3D coreless filament winding technology. *Journal of Composite Materials*, 2018.

[14] Niklas Minsch, Matthias Müller, Thomas Gereke, Andreas Nocke, and Chokri Cherif. 3D truss structures with coreless 3D filament winding technology. *Journal of Composite Materials*, 2019.

[15] Marshall Prado, Moritz Dörstelmann, Tobias Schwinn, Achim Menges, and Jan Knippers. Coreless filament winding. In *Robotic Fabrication in Architecture, Art and Design 2014*. Springer, 2014.

[16] Linwei He, Matthew Gilbert, and Xingyi Song. A Python script for adaptive layout optimization of trusses. *Structural and Multidisciplinary Optimization*, 2019.

[17] Alemseged Gebrehiwot Weldeyesus, Jacek Gondzio, Linwei He, Matthew Gilbert, Paul Shepherd, and Andrew Tyas. Adaptive solution of truss layout optimization problems with global stability constraints. *Structural and Multidisciplinary Optimization*, 2019.

[18] William F Baker, Lauren L Beghini, Arkadiusz Mazurek, Juan Carrion, and Alessandro Beghini. Structural innovation: combining classic theories with new technologies. *Engineering Journal-American Institute of Steel Construction*, 2015.

[19] Ozlem Comakli Sokmen, Seyma Emec, Mustafa Yilmaz, and Gokay Akkaya. An overview of Chinese Postman Problem. In *3rd International Conference on Advanced Engineering Technologies*, 2019.

[20] Horst A Eiselt, Michel Gendreau, and Gilbert La-
porte. Arc routing problems, part ii: The rural post-
man problem. *Operations research*, 1995.

[21] Saverio Spadea, John Orr, and Kristin Ivanova.
Bend-strength of novel filament wound shear rein-
forcement. *Composite Structures*, 2017.